

DETC2018-85859

## EXPERIMENTAL PERFORMANCE VERIFICATION OF A SYNCHRONIZATION BASED STATE OBSERVER USING ONLY COLLISION TIME INFORMATION

**Pascal V. Preiswerk\***

Institute for Nonlinear Mechanics  
University of Stuttgart  
Pfaffenwaldring 9, 70569 Stuttgart  
Email: preiswerk@inm.uni-stuttgart.de

**Remco I. Leine**

Institute for Nonlinear Mechanics  
University of Stuttgart  
Pfaffenwaldring 9, 70569 Stuttgart  
Email: leine@inm.uni-stuttgart.de

### ABSTRACT

*A state observer that only uses the collision time information has recently been developed for linear time-invariant multi-body systems with unilateral constraints. The observer is based on synchronization and makes use of switched geometric unilateral constraints, which generate a unidirectional coupling in a master-slave setup. In presence of uncertainties, such as model inaccuracies or disturbances, an exact reconstruction of the observed state is not possible. As a first step in assessing the robustness of the proposed observer, we present an experimental verification of the observer's performance. Furthermore, we account for dry friction in the observer design.*

### INTRODUCTION

Various state observer designs have been proposed in the literature for different classes of non-smooth systems [4,5,9], most of which require continuous measurement signals as input for the observer. In [2], a state observer design that only requires the collision time information in form of a boolean function was presented. Therein, the concept of switched unilateral constraints is introduced, which allows the collision time information to act as a unidirectional coupling between two systems in a master-slave setup. This type of coupling leads to synchronization of the two systems and can therefore be used for designing a state observer. However, just as some widely used state observers for smooth systems, such as the Luenberger observer [8], this type of syn-

chronization based state observer is depending on an accurate mathematical model of the observed system. Synchronization cannot be achieved in the presence of model inaccuracies and disturbances and therefore an exact reconstruction of the observed state is not possible. Therefore, the robustness of the proposed state observer against such disturbances has to be investigated. As a first step, the current paper gives an experimental proof-of-concept of the synchronization based observer design for a vibro-impact system using only collision time information.

### SYNCHRONIZATION BASED STATE OBSERVER

In the following, we briefly review the basic concepts of the synchronization based state observer design presented in [2], and, in addition, extend the observer to account for dry friction. Consider a non-smooth mechanical system consisting of a linear, time-invariant structure subjected to geometric unilateral constraints (leading to impacts) and non-opening frictional contacts. The system under consideration is typically a vibro-impact system with frictional linear guides. Let  $\mathbf{q}(t)$  be the generalized coordinates parametrized by the time  $t$  and let  $\mathbf{u}(t)$  denote the corresponding generalized velocities. The non-impulsive dynamics is described by

$$\begin{aligned} \dot{\mathbf{q}} &= \mathbf{u} \\ \mathbf{M}\dot{\mathbf{u}} + \mathbf{C}\mathbf{u} + \mathbf{K}\mathbf{q} &= \mathbf{W}\boldsymbol{\lambda} + \mathbf{W}_T\boldsymbol{\lambda}_T + \mathbf{f}(t), \end{aligned} \quad (1)$$

\*Address all correspondence to this author.

where the system matrices  $\mathbf{K} = \mathbf{K}^T \succ 0$ ,  $\mathbf{M} = \mathbf{M}^T \succ 0$  and  $\mathbf{C} \succ 0$  are assumed to be constant and positive definite, and the matrices  $\mathbf{W}$  and  $\mathbf{W}_T$  are constant. The contact forces  $\boldsymbol{\lambda}$  model the non-impulsive constraint forces of the unilateral constraints, whereas the contact forces  $\boldsymbol{\lambda}_T$  model the friction forces in non-opening contacts. The matrix  $\mathbf{W}$  is composed of the generalized force directions of each unilateral constraint and the matrix  $\mathbf{W}_T$  contains the generalized force directions of the non-opening frictional contacts. The system is excited by an external forcing  $\mathbf{f}(t)$ . The impact equations at collision time  $t_c$  are given by

$$\mathbf{M}(\mathbf{u}^+(t_c) - \mathbf{u}^-(t_c)) = \mathbf{W}\boldsymbol{\Lambda}(t_c), \quad (2)$$

with the impulsive forces  $\boldsymbol{\Lambda}$  of the unilateral constraints. In order to formulate set-valued force laws, we will make use of the following set valued functions: The unilateral primitive [6]

$$\text{Upr}(x) = \begin{cases} 0 & \text{if } x > 0 \\ [-\infty, 0] & \text{if } x = 0 \\ \emptyset & \text{if } x < 0, \end{cases} \quad (3)$$

used to describe unilateral constraints, and the set-valued sign function

$$\text{Sign}(x) = \begin{cases} 1 & \text{if } x > 0 \\ [-1, 1] & \text{if } x = 0 \\ -1 & \text{if } x < 0, \end{cases} \quad (4)$$

used for the description of the friction forces. Let the friction forces  $\boldsymbol{\lambda}_T$  obey the Coulomb-type friction law

$$-\lambda_{Ti} \in \mu_i \lambda_{Ni} \text{Sign}(\gamma_{Ti}), \quad (5)$$

with known normal forces  $\lambda_{Ni}$  at the frictional contacts and friction coefficients  $\mu_i$ . By  $\gamma_{Ti}$  we denote the elements of the relative tangential contact velocity for frictional contacts, given by  $\boldsymbol{\gamma}_T = \mathbf{W}_T^T \mathbf{u}$ . Furthermore, assume that there exist boolean switching functions  $\chi_i(t)$ , taking values  $\chi_i(t) \in \{0, 1\}$ , such that the contact forces  $\boldsymbol{\lambda}$  are governed element wise by

$$-\lambda_i \in \begin{cases} \text{Upr}(\gamma_i) & \text{if } \chi_i(t) = 1 \\ 0 & \text{if } \chi_i(t) = 0, \end{cases} \quad (6)$$

a force law referred to as switched geometric unilateral constraint. Note that for a geometric unilateral constraint the switching function  $\chi_i(t)$  is given by

$$\chi_i(t) = \begin{cases} 1 & \text{if } g_i = 0 \\ 0 & \text{if } g_i > 0, \end{cases} \quad (7)$$

where  $g_i(\mathbf{q})$  is the contact distance of the  $i^{\text{th}}$  unilateral constraint. Upon collision, the impulsive forces  $\boldsymbol{\Lambda}$  of the closed unilateral constraints are defined by an impact law of the form

$$-\boldsymbol{\Lambda} \in \mathcal{H}(\bar{\boldsymbol{\gamma}}), \quad (8)$$

where  $\mathcal{H} : \mathbb{R}^n \rightrightarrows \mathbb{R}^n$  is assumed to be a maximal monotone, set-valued operator and  $\bar{\boldsymbol{\gamma}} = \frac{1}{2}(\boldsymbol{\gamma}^+ + \boldsymbol{\gamma}^-)$  with the relative contact velocities  $\boldsymbol{\gamma}$ . As shown in [2, 10], impact laws such as the generalized Newton's impact law or the generalized Poisson's impact law can be written in the form (8) with  $\mathcal{H}$  being maximal monotone.

Now that we have established the type of system under consideration, our goal is to design a state observer that only relies on the impact time information. The idea is to consider two identical systems, defined by the equations (1)-(2), in a master-slave setup and to introduce a unidirectional coupling between the two systems that will lead to synchronization. In other words, as time tends to infinity, the state of the slave system, which represents the state observer, will become identical to the state of the master system, which represents the observed plant. In fact, the boolean switching function  $\chi(t)$  can be used to generate the desired coupling between the two systems. Consider a master system of the form (1)-(2) and an identical slave system, both under the additional assumption that the columns of  $\mathbf{W}$  are linearly independent. The state of the master system is denoted with a subscript  $m$ , whereas the state of the slave system is denoted with a subscript  $s$ . The two systems synchronize, if the error dynamics of the state difference between the two systems is asymptotically stable. Let  $(\mathbf{q}_m(t), \mathbf{u}_m(t))$  and  $(\mathbf{q}_s(t), \mathbf{u}_s(t))$  be two arbitrary solutions of the two systems. By denoting the state difference as  $\mathbf{e}_q = \mathbf{q}_m - \mathbf{q}_s$  and  $\mathbf{e}_u = \mathbf{u}_m - \mathbf{u}_s$  and using equations (1) and (2), the error dynamics can be written as

$$\mathbf{M}\dot{\mathbf{e}}_u + \mathbf{C}\mathbf{e}_u + \mathbf{K}\mathbf{e}_q = \mathbf{W}(\boldsymbol{\lambda}_m - \boldsymbol{\lambda}_s) + \mathbf{W}_T(\boldsymbol{\lambda}_{Tm} - \boldsymbol{\lambda}_{Ts}) \quad (9)$$

in the non-impacting phase and

$$\mathbf{M}(\mathbf{e}_u^+ - \mathbf{e}_u^-) = \mathbf{W}(\boldsymbol{\Lambda}_m - \boldsymbol{\Lambda}_s) \quad (10)$$

at the impact time instants. We show stability of the error dynamics by introducing the positive definite Lyapunov function

$$V = \frac{1}{2} (\mathbf{e}_u^T \mathbf{M} \mathbf{e}_u + \mathbf{e}_q^T \mathbf{K} \mathbf{e}_q) \quad (11)$$

and showing that the time derivative  $\dot{V}(\mathbf{e}_q, \mathbf{e}_u)$  and jumps at impact times  $V^+ - V^- := V(\mathbf{e}_q^+, \mathbf{e}_u^+) - V(\mathbf{e}_q^-, \mathbf{e}_u^-)$  are both negative

semidefinite. The time derivative of the Lyapunov function evaluated along solutions of the error dynamics equates to

$$\begin{aligned}\dot{V} &= \mathbf{e}_u^T \mathbf{M} \dot{\mathbf{e}}_u + \mathbf{e}_q^T \mathbf{K} \dot{\mathbf{e}}_q \\ &= \mathbf{e}_u^T (-\mathbf{C} \mathbf{e}_u + \mathbf{W}(\boldsymbol{\lambda}_m - \boldsymbol{\lambda}_s) + \mathbf{W}_T(\boldsymbol{\lambda}_{Tm} - \boldsymbol{\lambda}_{Ts})) \\ &= -\mathbf{e}_u^T \mathbf{C} \mathbf{e}_u + (\boldsymbol{\gamma}_m - \boldsymbol{\gamma}_s)^T (\boldsymbol{\lambda}_m - \boldsymbol{\lambda}_s) \\ &\quad + (\boldsymbol{\gamma}_{Tm} - \boldsymbol{\gamma}_{Ts})^T (\boldsymbol{\lambda}_{Tm} - \boldsymbol{\lambda}_{Ts}),\end{aligned}\quad (12)$$

where  $-\mathbf{e}_u^T \mathbf{C} \mathbf{e}_u \leq 0$  due to the positive definiteness of  $\mathbf{C}$ ,  $(\boldsymbol{\gamma}_m - \boldsymbol{\gamma}_s)^T (\boldsymbol{\lambda}_m - \boldsymbol{\lambda}_s) \leq 0$  due to the monotonicity of the force law (6) and  $(\boldsymbol{\gamma}_{Tm} - \boldsymbol{\gamma}_{Ts})^T (\boldsymbol{\lambda}_{Tm} - \boldsymbol{\lambda}_{Ts}) \leq 0$  due to the monotonicity of the friction law (5) (see [7]).

The velocity jumps at the impact time instants induce a jump of the Lyapunov function which is obtained as

$$\begin{aligned}V^+ - V^- &= \frac{1}{2}(\mathbf{e}_u^+ + \mathbf{e}_u^-)^T \mathbf{M}(\mathbf{e}_u^+ - \mathbf{e}_u^-) \\ &= (\tilde{\boldsymbol{\gamma}}_m - \tilde{\boldsymbol{\gamma}}_s)^T (\boldsymbol{\Lambda}_m - \boldsymbol{\Lambda}_s),\end{aligned}\quad (13)$$

being negative semidefinite since the impact law (8) is maximal monotone. Hence, the Lyapunov function cannot increase at any time, which proves uniform stability of the origin [7]. Under the assumption that the unilateral constraints cannot remain closed for an infinite amount of time, the origin is moreover globally uniformly asymptotically stable for systems without friction, as proven in [2]. For systems with non-opening frictional contacts and a maximal monotone friction force law, as considered here, global asymptotic stability is expected to be achieved under the assumption that the friction contacts cannot remain in a stick phase for an infinite amount of time. Given the asymptotic stability of the error dynamics, the slave system can be used as a state observer for a real system: the observed real system, acting as the master system, is subjected to geometric unilateral constraints which generate the switching functions  $\boldsymbol{\chi}(t)$  for the slave system. More precisely, by defining the switching functions of the slave system as

$$\chi_i(t) = \begin{cases} 1 & \text{if } g_i(\mathbf{q}_m) = 0 \\ 0 & \text{if } g_i(\mathbf{q}_m) > 0, \end{cases}\quad (14)$$

the observer state  $(\mathbf{q}_s, \mathbf{u}_s)$  is synchronizing with the state  $(\mathbf{q}_m, \mathbf{u}_m)$  of the observed real system.

The synchronization speed can be increased by allowing for position jumps for the slave system whenever an impact occurs in the master system, as shown in [1]. Furthermore, the observer can be extended to systems where  $\mathbf{K} = \mathbf{K}^T$  and  $\mathbf{C}$  are positive semidefinite such that the system is allowed to undergo a free rigid body motion (without any coupling to the environment).

As an example, consider the two degrees of freedom oscillator shown in Figure 1, which is a model of the experimental setup that we are using. Two masses,  $m_1$  and  $m_2$ , are coupled with the environment by a spring-damper element each. In addition, the two masses are connected by a spring with stiffness  $k_2$ . Dry friction is acting in the non-opening contacts between the masses and the support. Mass  $m_1$  is forced by an external excitation force  $F(t)$  acting in the direction of movement. Mass  $m_2$  is subjected to a geometric unilateral constraint in the real setup (acting as the master system). The slave system is subjected to a switched geometric unilateral constraint, whose switching function  $\boldsymbol{\chi}(t)$  is generated by the master system in the sense of (14). Note that the proof of asymptotic stability of the error dynamics is not yet complete for systems with dry friction. However, since friction is present in our experimental setup, we include friction in the model and investigate experimentally if the observer provides a satisfactory state estimation in the presence of friction.

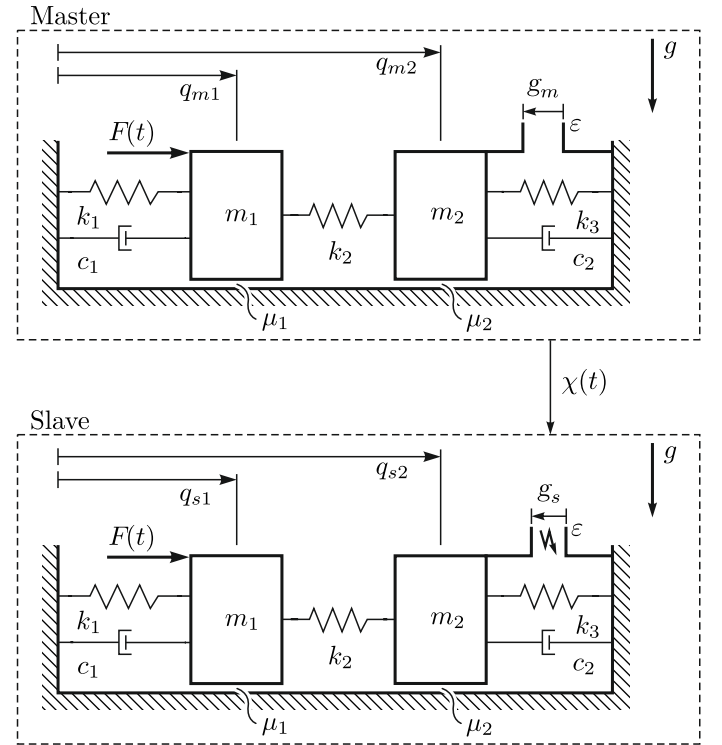


**FIGURE 1.** Model of the experimental setup in a master-slave setting: the switching function  $\boldsymbol{\chi}(t)$  is generated by the master system and builds the unidirectional coupling required for synchronization. The lightning symbol in the slave system indicates that the unilateral constraint is activated by a switching function  $\boldsymbol{\chi}(t)$  and that position jumps are used to instantly set the contact distance  $g_s$  to zero in case of an impact.

## EXPERIMENTAL RESULTS

As a first step in evaluating the robustness of the proposed synchronization based state observer, we evaluate the observer performance for a simple mass-spring-damper setup. Specifically, we compare the observer output to the measured state and to a simulation that receives the measured excitation force as an input, but does not receive the impact time information and hence is not coupled to the master system.

### Experimental Setup

We implement a synchronization based state observer for a simple mass-spring system. The setup consists of two steel blocks, each mounted on a cart of a linear roller guide, as shown in Figure 2. Each cart is attached to four linear coil tension springs that connect the carts to both ends of the linear guide as well as to each other. All springs are under pretension to prevent buckling during operation. A unilateral constraint is implemented as a limiting stop in form of a massive aluminium block that can be positioned at various locations on the linear guide. In order to reduce plastic deformation due to the impulsive impact forces, two tempered steel support pins are installed in the contact points of both, mass 2 and the block. One of the support pins is electrically isolated from the rest of the setup, such that contact between the support pins can be detected by applying a DC voltage between them: both pins are part of an open electric circuit. When contact occurs, the circuit closes and the voltage between the two pins drops to zero. This voltage measurement signal is then used to generate the switching function  $\chi(t)$  which is a required input for the state observer. For the assessment of the performance of the state observer, the velocities and positions of both masses are measured with two laser Doppler vibrometers. While one laser is pointing directly to mass 2 through bores in the surrounding parts, an extension beam is used for mass 1 because of spacial restrictions. Finally, an electrodynamic shaker induces an excitation force on mass 1. The excitation force, which is also a required input for the state observer, is measured with a piezoelectric force sensor mounted on mass 1, being connected to the shaker over a stinger. An internal highpass filter in the data acquisition hardware acting on the force measurement signal is inverted during signal processing. However, the 0.5 Hz cut-off frequency of the first order highpass filter causes a difference between the measured and the reconstructed force of only about 2% of the measured excitation force.

### Model

The experimental setup is modeled as a two degrees of freedom oscillator shown in Figure 1. One damping element is acting on each mass. However, a damping element between the two masses has been omitted after parameter identification measurements suggested a vanishing intermediate damping coefficient. The dynamics of the setup model is described by equations (1)-

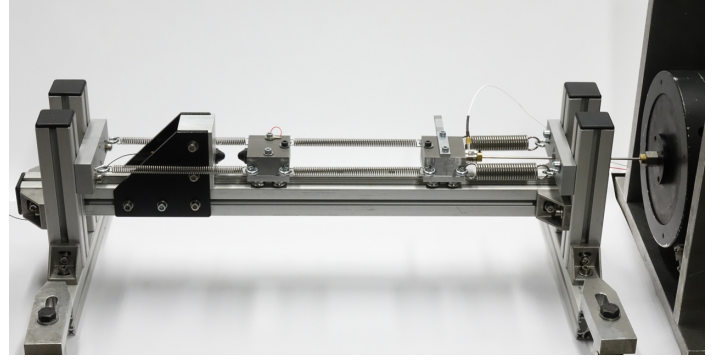


**FIGURE 2.** The experimental setup. Two masses on a linear roller guide are connected to prestressed coil springs.

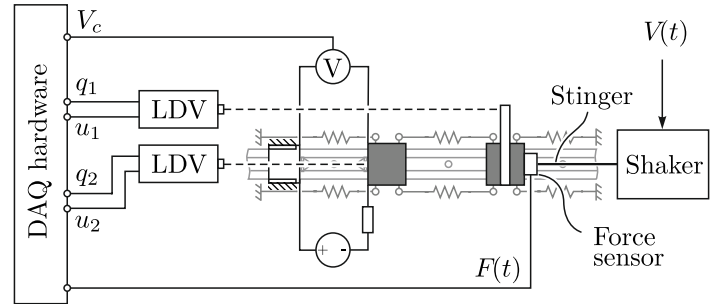


**FIGURE 3.** Schematic measurement setup. Two laser Doppler vibrometers (LDV) measure the positions and velocities of the two masses. Contact is detected by measuring the voltage between mass 2 and the stop. Furthermore, a piezoelectric force sensor measures the excitation force which is applied by an electrodynamic shaker.

(2) with

$$\mathbf{M} = \begin{pmatrix} m_1 & 0 \\ 0 & m_2 \end{pmatrix}, \mathbf{C} = \begin{pmatrix} c_1 & 0 \\ 0 & c_2 \end{pmatrix}, \mathbf{K} = \begin{pmatrix} k_1 + k_2 & -k_2 \\ -k_2 & k_2 + k_3 \end{pmatrix} \quad (15)$$

$$\mathbf{W} = \begin{pmatrix} 0 \\ -1 \end{pmatrix}, \mathbf{W}_T = \begin{pmatrix} -1 & 0 \\ 0 & -1 \end{pmatrix} \text{ and } \mathbf{f}(t) = \begin{pmatrix} F(t) \\ 0 \end{pmatrix}.$$

The generalized Newton's impact law is assumed, with a coefficient of restitution  $\varepsilon < 1$ , which yields a maximal monotone impact law. The model parameters for the experimental setup, which have been identified including linear experimental modal analysis techniques, are  $m_1 = 0.76 \text{ kg}$ ,  $m_2 = 0.696 \text{ kg}$ ,  $k_1 = 5283 \text{ N/m}$ ,  $k_2 = 981 \text{ N/m}$ ,  $k_3 = 970 \text{ N/m}$ ,  $c_1 = 1 \text{ Ns/m}$  and  $c_2 = 1.15 \text{ Ns/m}$ . In addition, the friction coefficients have been identified as  $\mu_1 = 0.04$  and  $\mu_2 = 0.035$  and the coefficient of restitution as  $\varepsilon = 0.1$ .

## Results

We generate a non-periodic motion by feeding a harmonic input voltage signal with a modulated amplitude and frequency to the excitation shaker. The resulting excitation force acting on the setup is generally non-harmonic, since it is affected by various non-modeled influences such as the shaker internal dynamics. The input voltage signal is of the form

$$V(t) = a(t) \sin(\omega(t) \cdot t), \quad (16)$$

with a randomly continuously modulated amplitude in the range  $a(t) \in [2.5, 5]V$  and frequency in the range  $\omega(t) \in [12\pi, 20\pi] \frac{\text{rad}}{\text{s}}$ . The system's state and the excitation force are measured over a time interval of 130 s and all measurement signals are sampled at 20 kHz. The output of the state observer, i.e. the simulation using the measured excitation force and impact time instants as inputs, is then compared to a simulation of the model that uses only the measured excitation force as input, which will simply be referred to as "simulation". The state observer output shows a better fit with the measurement data compared to the simulation: for correct initial conditions  $\mathbf{q}_0 = \mathbf{u}_0 = \mathbf{0}$ , the mean observer position error is at 2.9 % of the maximum deflection and the mean observer velocity error is at 2.4 % of the maximum velocity. Hence the state observer does not perfectly synchronize with the measured state, which is a result of model uncertainties and measurement errors. For the simulation, the mean position error is at 8.5 % of the maximum deflection and the mean velocity error is at 6.8 % of the maximum velocity. However, looking at the time evolution, the simulation shows an alternation of time intervals with a good match and time intervals with a poor match between measurement and simulation, whereas the observer matches fairly well with the measurement over the entire measured time interval. Figure 4 shows the typical pattern for a selected time interval. After an instant of good match for both, the observer and the simulation, the simulation temporarily diverges from the measured state, while the state observer output stays in the vicinity of the measured state at all times. This can also be seen from the Euclidean position and velocity observer error in Figure 5.

Small mismatches in the collision time instants between the setup and the state observer, caused for example by insufficient exactness of the collision time measurement, or by the fact that velocity jumps are not perfectly instantaneous in reality, lead to a high pointwise error in the velocities near the collision time instants. This phenomenon is known as "peaking" (see for instance [3]). Additionally, small phase mismatches between the measurement and the simulation can cause high pointwise estimation errors. Therefore, an improved error measure has to be introduced in order to achieve a more meaningful quantitative analysis of the estimation error.

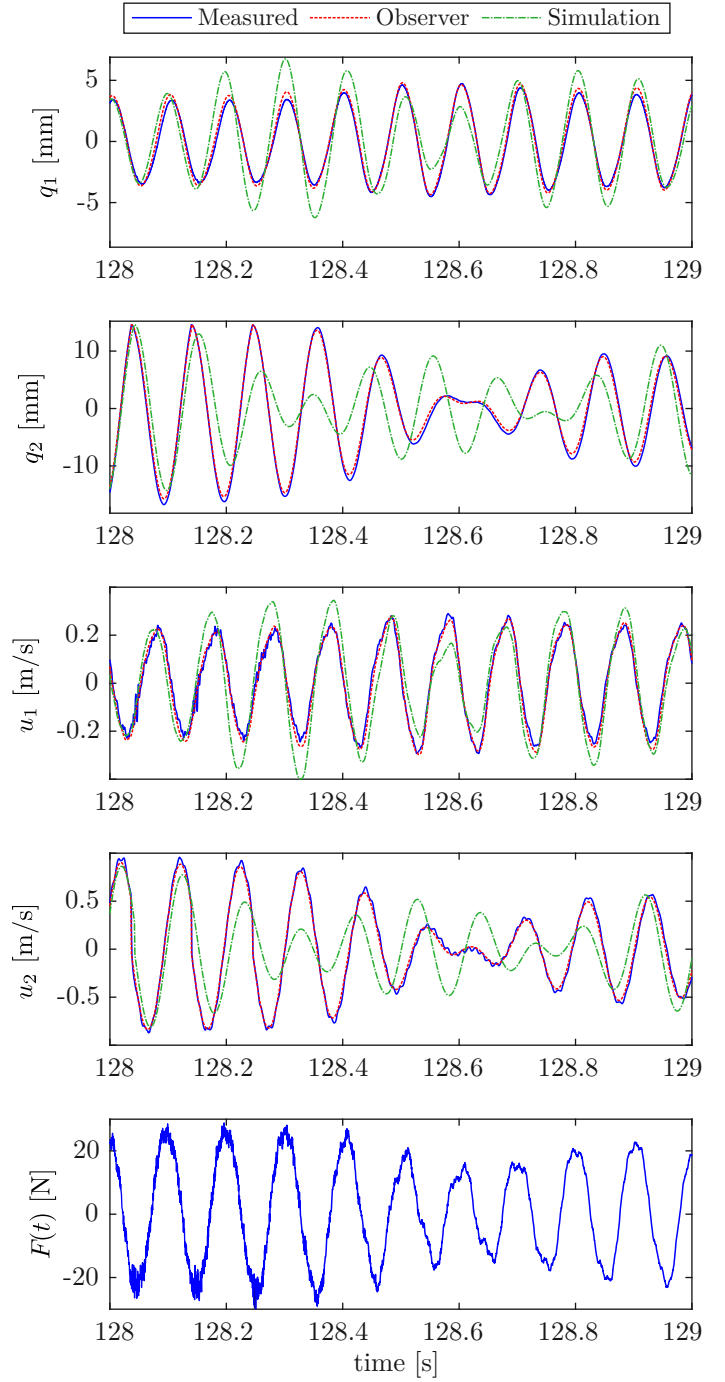


**FIGURE 4.** Extract from the time evolution of the positions  $(q_1, q_2)$  and velocities  $(u_1, u_2)$  from the measurement signals (blue), the observer output (dashed red) and the simulation that only uses the excitation force as an input (dashed green). The observer output is almost overlapping the measured signal. Also shown is the measured excitation force  $F(t)$ .

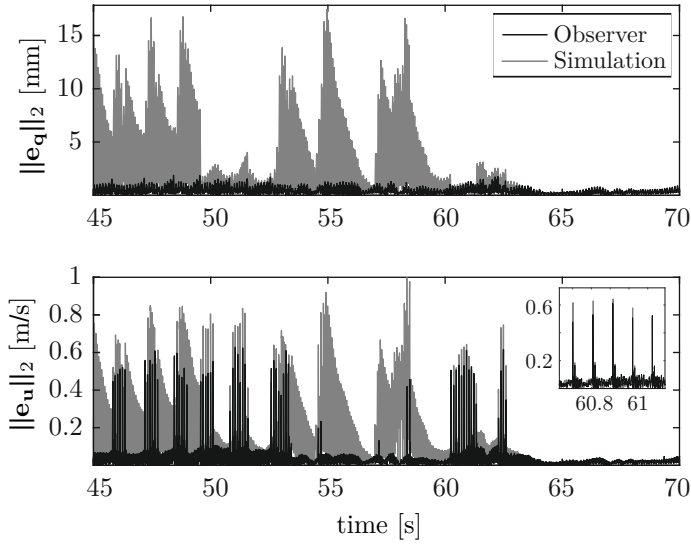


**FIGURE 5.** Euclidean position and velocity estimation error in a selected representative time interval. The velocity error exhibits peaking near collision time instants.

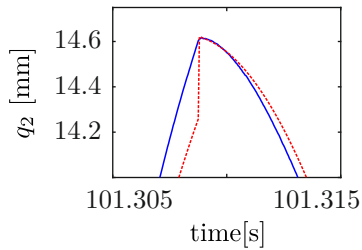


**FIGURE 6.** Close-up of a kink in the position  $q_2$  for the measured signal (blue) and a jump in the observer estimation (red) near a collision time instant. Since the observer does not perfectly synchronize with the experimental setup due to model inaccuracies, the observer position jumps at impact time instants regularly reduce the estimation error.

The observer position jumps at the impact time instants do not only lead to an increased synchronization speed but they correct a part of the discrepancies caused by the model inaccuracies, as shown in Figure 6. However, the observer's pre-impact contact distance provides additional information that has not yet been exploited, but could for example be utilized in adaptive parameter and model updating strategies.

## Conclusion

The presented synchronization based state observer shows a good match with the measured state in an experimental setup, compared to a simulation that does not use the collision time information as an input. The state observer output follows the real

state under a slowly varying harmonic excitation that changes both amplitude and frequency, while a simulation of the system using only the measurement of the excitation force alternates between phases of good match and phases of poor state estimation. For a more meaningful quantitative evaluation of the estimation error, an improved error measure has to be introduced, that can eliminate the peaking caused by slight mismatches in the collision time instant. Letting the observer's position state jump at collision time instants helps to increase the synchronization speed and corrects the position of the colliding body whenever an impact occurs. However, the measured collision time instants contain additional information that has not yet been used: the value of the observer's pre-impact contact distance provides a measure of how closely synchronized the master and the slave system are and could be used in adaptive parameter and model updating strategies.

## REFERENCES

- [1] BAUMANN, M., AND LEINE, R. I. Synchronization-based state observer including position jumps for impacting multibody systems. In *Proceedings of the 2015 IEEE 54th Annual Conference on Decision and Control (CDC)* (2015).
- [2] BAUMANN, M., AND LEINE, R. I. A synchronization-based state observer for impact oscillators using only collision time information. *International Journal of Robust and Nonlinear Control*, 26 (2016), 2542–2563.
- [3] BIEMOND, J., HEEMELS, W., SANFELICE, R., AND VAN DE WOUW, N. Distance function design and Lyapunov techniques for the stability of hybrid trajectories. In *Automatica* 73 (2016), pp. 38–46.
- [4] BROGLIATO, B., AND HEEMELS, W. P. M. H. Observer design for Lur'e systems with multivalued mappings: a passivity approach. *IEEE Transactions on Automatic Control* 54, 8 (2009), 1996–2001.
- [5] DORIS, A., JULOSKI, A. L., MIHAJLOVIC, N., HEEMELS, W. P. M. H., VAN DE WOUW, N., AND NIJMEIJER, H. Observer designs for experimental non-smooth and discontinuous systems. *IEEE Transactions on Control Systems Technology* 16, 6 (2008), 1323–1332.
- [6] GLOCKER, CH. *Set-valued Force Laws, Dynamics of Non-smooth Systems*, vol. 1 of *Lecture Notes in Applied Mechanics*. Springer-Verlag, 2001.
- [7] LEINE, R. I., AND VAN DE WOUW, N. *Stability and Convergence of Mechanical Systems with Unilateral Constraints*, vol. 36 of *Lecture Notes in Applied and Computational Mechanics*. Springer Verlag, Berlin, 2008.
- [8] LUENBERGER, D. G. Observers for multivariable systems. *IEEE Transactions on Automatic Control* 11, 2 (1966), 190 – 197.

- [9] PAVLOV, A., POGROMSKY, A. Y., VAN DE WOUW, N., AND NIJMEIJER, H. On convergence properties of piecewise affine systems. *International Journal of Control* 80, 8 (2007), 1233–1247.
- [10] WINANDY, T., BAUMANN, M., AND LEINE, R. I. Variational analysis of inequality impact laws for perfect unilateral constraints. In *Advanced Topics in Nonsmooth Dynamics*, R. I. Leine, V. Acary, and O. Brils, Eds., Transactions of the European Network for Nonsmooth Dynamics. Springer, 2018, in press, ch. 2.